Biocompatible Glycine-Assisted Catalysis of the Sol-Gel Process: Development of Cell-Embedded Hydrogels

Laurine Valot, Marie Maumus, Titouan Montheil, Jean Martinez, Daniele Noel, Ahmad Mehdi, Gilles Subra

Biocompatible Glycine-Assisted Catalysis of the Sol-Gel Process: Development of Cell-Embedded Hydrogels

Laurine Valot,[a,b] Marie Maumus,[c] Titouan Montheil,[a] Jean Martinez,[a] Danièle Noël,[c] Ahmad Mehdi*[b] and Gilles Subra*[a]

Abstract: Sol-gel can be used for hydrogel cross-linking, opening an attractive route to design biocompatible hydrogels in soft conditions. Sol-gel can be catalysed at basic and acidic pH or around neutrality with the addition of a nucleophile. Therefore, working around pH 7, unlocks the possibility of direct cell embedment and the preparation of bioinks. With the aim of proposing a generic method for sol-gel 3D bioprinting, we first screened different nucleophilic catalysts using bis-silylated polyethylene glycol (PEG) as a model hydrogel. A synergistic effect of glycine and NaF, used in low concertation to avoid any toxicity, was pointed out. Biocompatibility of the approach was demonstrated by embedding primary mouse mesenchymal stem cells. The measure of viscosity as a function of time showed the impact of reaction parameters on the kinetics of the sol-gel process, such as temperature, complexity of the medium, pH and cells addition, to predict the gelation time.

Introduction

Hydrogels play a central role in the field of biomedical materials. Indeed, their high water content is a key feature to mimic the extracellular matrix, and a prerequisite for cell encapsulation. Most of the cell-containing bioinks used for 3D bioprinting, are physical hydrogels assembled through weak interactions. Only very few of them are chemical hydrogels reticulated through covalent bonds. They were obtained by click chemistry (e.g. Michael addition, Schiff-base reaction, aldehyde-hydrazide ligation), photo-polymerization and enzymatic reactions.[1–9] In that context we have developed the sol-gel inorganic polymerization as a new method for 3D printing.[10] Sol-gel is a well-known process[11–14] allowing the preparation of oxides or hybrid materials in soft conditions. Hydrolysis and condensation of alkoxysilanes may proceed in water, in a chemoselective way, and can be considered as a bioorthogonal reaction. Interestingly, as far as one alkoxysilyl group is introduced on a biomolecule, the resulting silylated 'hybrid block' can be combined with other hybrid biomolecules to afford bioactive hydrogels in one-step. For instance, bis-silylated polyethylene glycol can be used as elementary building block to establish the 3D network, while ~10 m% of mono-functionalised bioactive peptides will afford the desired biological properties to the hydrogel.[15] We have also demonstrated that short peptide sequences inspired from collagen could also be used to obtain hydrogels in which cells can be embedded.[16] However, only few examples of sol-gel process hydrogels applied to 3D-printing have been published, most of the time incompatible with cell encapsulation due to reaction conditions (acidic conditions or use of toxic catalysts).[10,17,18]

The main complexity of using bioink based on chemical hydrogel is to control its viscosity, as it increases simultaneously with the reticulation. For this reason, a suitable 'printing window' has to be determined, i.e. a period when the viscosity is sufficient to print with retention of the shape and without flowing, For extrusion printing, this window should be comprised between 30 and 6.10^7 mPa.s, depending of the nozzle's size, shape and the type of extruder (e.g. endless screw, air compressor). In the sol-gel process, the gelation time is dependent on the catalyst. The sol-gel reaction can be acid or base-catalysed. Indeed, hydrolysis proceeds quickly at acidic and basic conditions, and is the slowest at pH 7. Condensation is faster at pH 1 and 10, slow at pH 2 and above pH 2, as well as in basic conditions. Combination of both experimental conditions allows the sol-gel reaction to happen faster at pH 1, 4 and 12, and is the slowest at pH 7 (Figure 1).[19] Unfortunately, working at physiological pH (i.e. between 7.2 and 7.8) is compulsory to encapsulate cells during the reaction course.

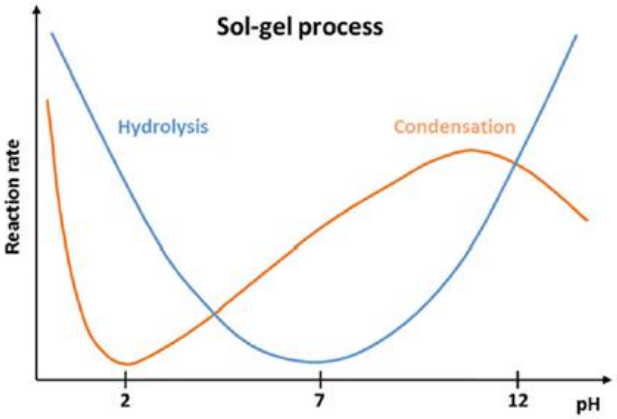

Figure 1. Reaction rates of tetraethyl orthosilicate hydrolysis (blue curve), and condensation (orange curve) as a function of pH.[19]

[a] Laurine Valot, Titouan Montheil, Pr. Jean Martinez and Pr. Gilles Subra
IBMM, Univ Montpellier, CNRS, ENSCM, Montpellier, France
gilles.subra@umontpellier.fr
[b] Laurine Valot and Pr. Ahmad Mehdi
ICGM, Univ Montpellier, CNRS, ENSCM, Montpellier, France
ahmad.mehdi@umontpellier.fr
[c] Dr. Marie Maumus and Dr. Danièle Noël
IRMB, Univ Montpellier, INSERM, CHU Montpellier, Montpellier, France

Supporting information for this article is given via a link at the end of the document.

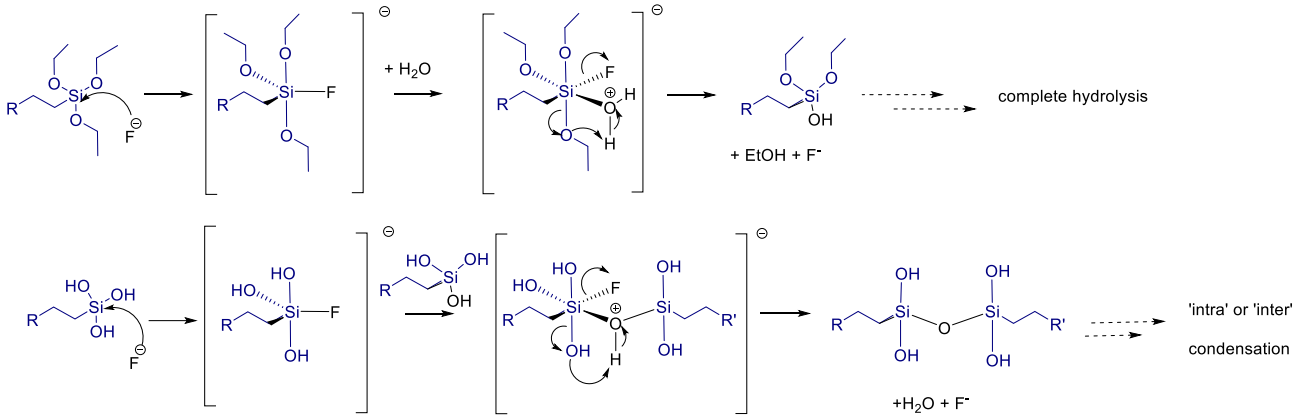

Scheme 1. Mechanism of F^- catalysed hydrolysis and condensation reactions in sol-gel hydrogel formation.

In order to overcome this limitation, a nucleophilic catalyst can be used. Sodium fluoride (NaF) is extensively applied for that purpose,[20] catalysing both hydrolysis and condensation (Scheme 1).[11,21–23] However, sodium fluoride is toxic for cells at a 24 mM concentration, which is usually required for efficient catalysis.[24–28] We thus searched for an alternate catalyst with low toxicity, and studied whether other reaction parameters could impact the sol-gel reaction.

Results and Discussion

Catalyst screening

As a model, we chose a hydrogel prepared from 10 wt% bis-silylated PEG **1** at 37 °C and pH 7.4, in DPBS buffer (Dulbecco's phosphate-buffered saline) (Scheme 2, see supporting information for the synthesis and analysis of compound **1**, Figure S1-S3, and hydrogel's preparation). With no catalysis, it took one week to reach the gelation. At 3 mg/mL (71.5 mM, 1.78 eq. related to PEG, i.e. 0.3 eq. per alkoxysilane function), NaF quickly catalysed formation of the covalent network. Indeed, the gel reached a 100 mPa.s viscosity (corresponding to a gel state) within 135 minutes. However, 53 hours were required to reach the same viscosity when using NaF at 0.1 mg/mL (2.38 mM).

Different catalysts were assayed, at the same concentration than NaF (71.5 mM). This first screening was performed by the 'tilting method', i.e. the gelation time was determined when the sample could not flow upon turning the vial upside down (Scheme 2). Results are presented in Table 1 (and Table S1).

Different fluoride salts including KF and TBAF (Tetra-n-butylammonium fluoride) were assayed and compared to NaF. The nature of the fluoride counter-ion had no influence; TBAF, NaF and KF inducing gelation around 2h30. As expected, solutions prepared with Na_2FPO_3 were less efficient, and turned into a gel after one day. Indeed, monofluorophosphate needed to be hydrolysed before yielding fluoride and hydrogen phosphate, but occurred slowly at pH 7.4. Besides, non-fluorinated salts like magnesium sulphate and calcium chloride were also inefficient.

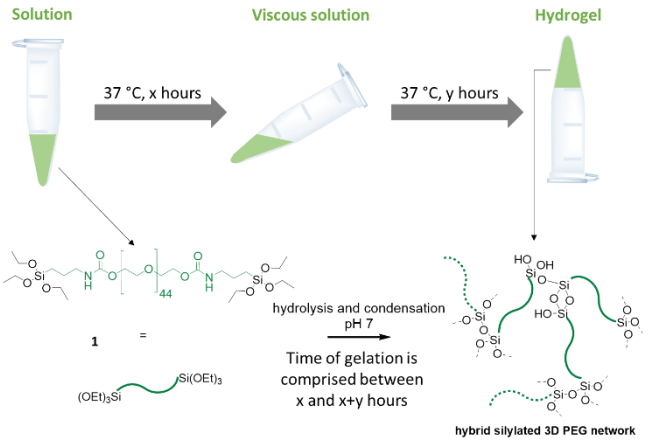

Scheme 2. Tilting method for gelation assessment of bis-silylated-PEG solutions.

Table 1. Tilting gelation assays of 10 wt% PEG hydrogels in DPBS (pH 7.4) at 37 °C, with various catalysts. Catalyst effectiveness was appreciated from the time to reach gelation: (- - -) more than 7 days; (- -) between 3 and 7 days: (-) between 48 and 72 hours; (+) between 24 and 48 hours; (+ +) between 8 and 24 hours; and (+ + +) less than 8 hours.

* The pH of these solutions needed to be adjusted to 7.4.

Class of Chemical	Chemical	Concentration (mM)	Catalyst effectiveness	Catalyst effectiveness in combination with 0.1 mg/mL of NaF
Solvent	DPBS		- - -	-
Fluoride donors	NaF	71.5 = 3 mg/mL	+ + +	
		23.8 = 1 mg/mL	+ + +	
		2.38 = 0.1 mg/mL	-	
	KF	71.5	+ + +	
	Na_2FPO_3	71.5	+	
		143	+ +	
	Tetrabutylammonium fluoride	71.5	+ + +	
Diols	Glycerol	71.5	- - -	
	Ethylene glycol	71.5	- - -	
		143	- -	-
	(-) Pinanediol	71.5	- - -	
	Catechol	71.5	- -	+ +
		143		+ +
	4 –tert-butylcathechol	71.5	- -	+
	Cafeic acid	71.5	- - -	
	3 –amino-1.2-propanediol *	71.5	- / - -	
	β-cyclodextrin	71.5	- -	
Amines and diamines	Pyridine	71.5	- -	-
	Ethylene diamine*	71.5	- / - -	
	1.3-diamonipropane*	71.5	- / - -	
	o-Phenylenediamine	71.5	- -	
Thiols	Mercaptophenol	71.5	- -	+
	Mercaptophenylacetic acid*	71.5	+ +	+ +
	Thiophenol	71.5	- -	+
Sugars and derivatives	D-Glucose	143	- -	- -
		715	- -	
	D-(+)Galactose	71.5	- - -	
		715	- -	
	Maltose	71.5	- -	
		715	- -	
	Sucrose	71.5	- - -	
		715	- -	
	D-(-)Ribose	71.5	- - -	
		143	- -	+
	D-(+)Mannose	71.5	- -	- -
		143	- -	- -
	Mannitol	71.5	- -	
		143	- -	-
		715	- -	
	Sorbitol	71.5	- -	
		715	- -	
	D-Gluconic acid*	71.5	- - -	
Amino acids and derivatives	Glycine	143	- -	+ +
		715	-	+ +
	β-Alanine	143	- -	+ +
	Lysine*	71.5	- / - -	
	Histidine	143	- -	+ +
	N-acetyl histidine	143	- - -	+ +
	Glutamine	143	- -	+ +
	Cysteine	71.5	- -	+
		715	-	+
	N-acetyl cysteine*	143	-	+
	L Cysteine ethyl ester*	71.5	- - -	+
	Homocysteine*	143	- -	+
	N-acetyl homocysteine*	143	-	+ +
	DOPA	71.5	- -	+
	N-acetyl-DOPA	71.5	- -	+ / + +
Salts	$MgSO_4$	10	- -	-
	$CaCl_2$	10	- - -	- - -
Silica precursors	$Si(OH)_4$ *	143	+ / + +	+ +
	$Si(OEt)_4$	143	-	+ +
	Colloidal silica (Ludox)	143		+ / -

Beside fluoride derivatives, organic nucleophiles such as amines[29–31] may catalyse the sol-gel process by favouring the hydrolysis and condensation.[11,32,33] Other organic compounds may also drive the assembly of precursors by forming complexes. This is the case of multifunctional compounds like diols[34], sugars[35–41] and amino acids,[35,42–46].

A panel of organic compounds, including those cited above, were selected. It is worth noting that pH had to be adjusted to 7.4 with certain compounds (e.g. amines, carboxylic acids, noted with an '*' in Table 1). Indeed, as already explained, the sol-gel process is base-catalysed, and reaction kinetics would be strongly accelerated at pH > 8. Several unprotected amino acids (e.g. His, Lys, Gln, Cys, Gly, DOPA, βAla) were assayed as zwitterions. N-acetyl amino acids and amino acids esters were also used to evaluate the influence of the N or C-termini functions on catalysis.

Unfortunately, all catalysts yielded gelation times higher than 53 hours, even when employed at 715 mM. Only mercaptophenylacetic acid (MPAA) gave interesting results with gelation around 21 hours at 71.5 mM. However, at this concentration, MPAA was highly toxic for murine mesenchymal stem cells (mMSCs, data not shown).

At last, addition of a silica source [e.g. $Si(OEt)_4$, $Si(OH)_4$] was experimented. We hypothesized that hydroxysilane-containing additives could increase the number of reticulation knots, speeding the establishment of a 3D network. Unfortunately, tetraethylorthosilicate (TEOS) was not able to reduce significantly the gelation time (more than 2.5 days instead of less than 2.5 days for NaF at 0.1 mg/ml) and led to lower cell viability (65% after 24h, Figure S4). Indeed, at a concentration of 240 mM (14.0 µL/mL), which corresponded to the maximal quantity released by the bis-silylated PEG **1,** ethanol had low toxicity on mMSCs. This was not the case when additional ethanol was released by hydrolysis of TEOS, increasing the concentration to 812 mM (47.4 µL/mL) and leading to a cell viability decreased by a factor of 1.3. Silicic acid does not have this disadvantage and was able to reduce the gelation time by 2.2 fold at 143 mM. However, its use proved to be tricky. First, the silicic acid solution should be neutralized prior to its utilization, and the solution presented a short lifespan before condensation, leading to a poor reproducibility between assays. At last, addition of a mineral charge induced significant changes in the nature of the hydrogel (tougher hydrogel) resulting in an additional level of complexity in the design of cell-encapsulating matrices.

Summing up, no single compound used as catalyst was found to match the efficiency of NaF while maintaining a good cell viability.

Co-catalysis with 0.1 mg/mL NaF

We considered that 0.1 mg/mL NaF (2.38 mM, 0.06 eq. compared to PEG) was an acceptable concentration for cell embedding. Indeed, mMSCs covered with such a hydrogel showed a good viability viability as indicated by the live/dead assay, which showed absence of dead red cells (Figure 2). It appeared however that the number of living cell (65 %) was lower in all conditions as compared to the positive control (TC-PS with only cell culture on top of cells) when measured by the CellTiterGlo assay (Figure 3). This was likely due to a lower cell proliferation in wells were the hydrogels recovered the cells, which possibly trapped them. Results with hydrogels without catalyst tended to prove this. However, this high cell viability in the presence of NaF was higher than the one in solution (Figure S5). One explanation could be that a large part of the fluoride was associated with silicon atoms as pentavalent species, being less available to interact with cells. Moreover, new culture medium was added regularly on top of the hydrogel, thus diluting again the fluoride concentration below 0.1 mg/mL.

However, when [NaF] = 0.1 mg/mL, the gelation proceeded slowly (>50 hours), which was not adapted to 3D bioprinting. For this reason, we have investigated the use of a co-catalyst with NaF (Table 1, last row).

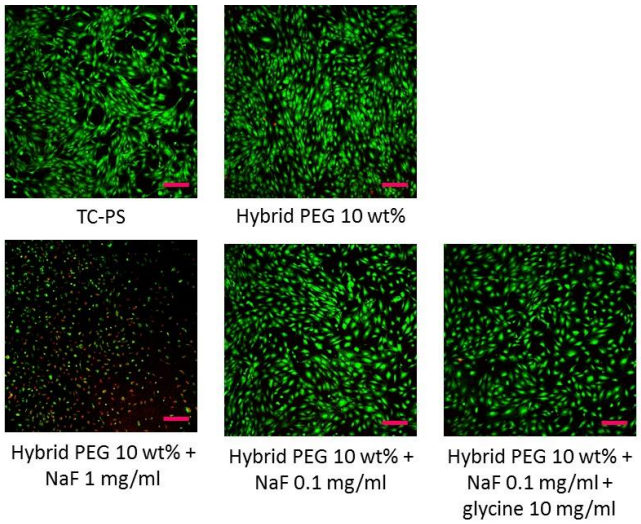

Figure 2. Cell viability of mMSCs measured by Live/Dead staining after 48 hours, covered with 10 wt% bis-silylated PEG hydrogel containing different amounts of catalyst. Scale bar 50 µm.

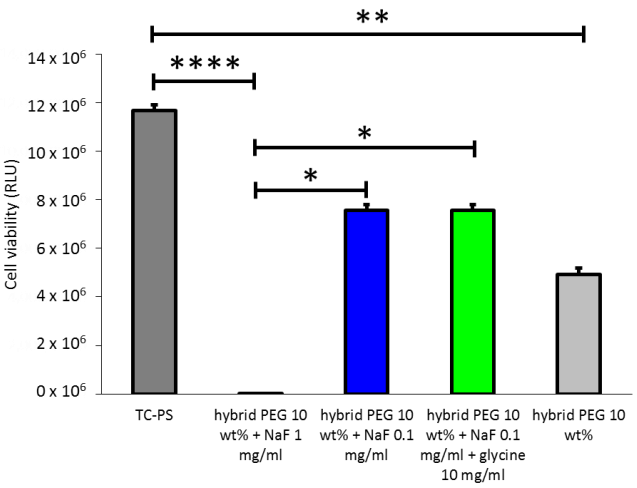

Figure 3. Cell viability of mMSCs covered with 10 wt% bis-silylated PEG hydrogel containing different amounts of catalyst. Measured by CellTiterGlo assay (RLU) after 48 hours.

Among all the assayed compounds, a large number of them (e.g. inorganic salts and sugars) did not improve the catalytic effect of NaF at 0.1 mg/mL. In contrast, the most effective diols, thiols and sugars (catechol, 4-tert-butylcatechol, L-DOPA, N-acetyl-DOPA, mercaptophenyl acetic acid and D-ribose used at 143 mM) reduced the gelation time by a factor of 1.4 to 3.7 (Table 1 and Table S2).

Addition of a mineral charge to NaF only improved modestly the kinetics, leading to a 1.3 to 2.6-fold reduction of the gelation time (for TEOS and $Si(OH)_4$, respectively).

The most interesting results were obtained with amino acids. All of them were able to reduce the gelation time by at least two folds. Moreover, they showed almost no toxicity even at high concentration (715 mM). It is worth noting that cysteine ethyl ester was less effective than cysteine, and so did N-acetyl histidine compared to unprotected histidine. These results tended to prove that both carboxylic acid and amino functions were implicated in the catalytic activity. The most interesting results were obtained with glutamine, histidine, N-acetyl-histidine, β–alanine and glycine, the later being the best one. In combination with 0.1 mg/ml NaF concentration, 143 mM and 715 mM H-Gly-OH concentrations reduced the gelation time to 17h30 and 12h respectively. It is worth to note that glycine is a very attractive additive, being abundant, achiral, non-toxic and highly soluble. For all these reasons, we selected it as co-catalyst for further studies. The biocompatibility of the catalyst mixture ([NaF] = 0.1 mg/ml and [H-Gly-OH] = 10 mg/ml) was evaluated. For doing so, mMSCs were seeded on culture plates and after 24h, they were covered with bis-silylated PEG hydrogel before gelation was reached. Cell viability was monitored at 48 hours by the Live/Dead assay and CellTiterGlo assay (Figure 2 and 3). As expected, addition of glycine did not impact on cell viability compared to hydrogel with NaF alone.

Proposed mechanism for NaF + Glycine catalysis

To get insights in the catalyst mechanism, liquid ^{29}Si NMR spectra were first recorded during gelation (10 wt% PEG-Si **1**, 0.1 mg/mL NaF and 10 mg/mL glycine in DPBS, see supporting information for protocol, Figure S6 and Table S3). Unfortunately, no signal shift associated to multivalent silicon conformation was observed (i.e. no signal between -60 and -90 ppm related to penta, hexa or heptavalent silicon[47]). This was most likely due to the long acquisition time for ^{29}Si NMR spectra (53 min) compared to the short lifetime of hyper coordinated complexes. On the other hand, the appearance of hydroxysilyl species was clearly observed after a few minutes indicating the beginning of hydrolysis. These species were not observed after 15 hours, showing that hydrolysis was complete. Thanks to the presence of a signal at -47.89 ppm, attributed to T^2 substructure i.e. mono-condensed species [RSi(OH)(OEt)-O-Si] after 3 hours, beginning of condensation was observed. As the condensation proceeded, polymeric species were formed and the resulting high molecular weight oligomers became insoluble, and were not observed anymore in the liquid state ^{29}Si NMR.

To understand if the addition of glycine impacted either hydrolysis or condensation, ^1H NMR (400 MHz) analyses were performed at different time points, in the presence of 0.1 mg/mL NaF alone or in combination with 10 mg/mL glycine, in DPBS and D_2O at 37 °C. We selected five characteristic protons for their vicinity with silicon atoms, which were integrated at different time points. We hypothesized that their signals could be impacted by hydrolysis and/or condensation (Figure 4A, 4B and S7). Signals of CH_2 and CH_3 of triethoxysilanes (q at 3.88 ppm in green and t at 1.24 ppm in dark blue) disappeared upon hydrolysis, and ethanol was released [q at 3.65 ppm (not shown because superposed to PEG signals and t at 1.18 ppm in light blue]. At the same time, the CH_2 in α position of silicone's triplet signals shifted from 0.74 ppm to 0.99 ppm (Figure 4, orange and red curves respectively). When condensation started, the polymeric species tended to become insoluble and this triplet signal decreased. This decrease was also observable on protons that were not directly impacted by hydrolysis (Figure S8).

We assumed that 50% of hydrolysis was obtained when 300 % of ethanol was released into the media (600 % was released at the end of hydrolysis because of the six ethoxy moieties). Strikingly, the time required to reach 50% of hydrolysis was decreased by six-fold upon addition of glycine (from 17h30 to 2h45), and the hydrolysis was complete after 15h while it required 70h with no glycine. Noteworthy, condensation also started earlier (6h *vs.* 28h), and went faster as indicated by the reduction of the CH_2 signal in α position of silicon.

Thus glycine co-catalysed both sol-gel hydrolysis and condensation. When the fluoride catalysis mechanism was described in the development of the sol-gel chemistry,[11,21–23] a putative mechanism of catalysis by primary amines was described by K. M. Delak and N. Sahai.[29,30] These authors reported that some amines (piperidine, ethylamine, imidazole and pyridine) at 0.915 mM concentration were able to catalyse both hydrolysis and condensation of trimethylethoxysilane, at pH of 5.5, proposing a nucleophile mechanism of reaction.[29,30] On the contrary, we have demonstrated that glycine alone was unable to catalyse the reaction even at high concentration. This was most likely due to working at physiological pH, and to the weak basic properties of glycine. Thus, we hypothesized that silicon was first activated by fluoride, yielding a pentacoordinated silicon intermediate.[48] Then, glycine might further complex the silicon yielding an heptacoordinate species thanks to the silicon ability to make up seven bonds. The zwitterion form of glycine (pKa = 2.3 for the carboxylic acid and 9.6 for the amine) could then form a five-atoms pseudo cycle upon elimination of ethanol (Scheme 3). We proposed that glycine also catalysed condensation by forming a complex with the hydroxide group and the silicon by weak binding, to reach a seven atoms pseudo cycle allowing its condensation with another trihydroxysilane.

To go further, methylamine and acetic acid, which can be viewed as mono functional analogues of glycine, were used as co-catalysts at the same concentration than glycine (133 mM), at pH 7.4. Using the tilting assay, acetic acid showed no significant co-catalytic activity while methylamine exerted comparable effects than glycine (between 15 and 23 hours to reach gelation). Moreover, when methylamine and acetic acid were used at the same time with NaF, the catalyst effect was less effective than that of glycine with NaF (gelation happened 3 hours later, comparable with the one of methylamine with NaF). As observed by ^{1}H NMR, the catalytic effect of methylamine improved the hydrolysis speed but was still less efficiently than glycine (Figure 4C). However, methylamine showed a limited impact on the condensation reaction. These results were in favour of the hypothesis of a concerted mechanism of catalyst involving both the amine and the carboxylic acid.

Some of our findings about the participation of both extremities of amino acid, were shared by the recent work of Kaβner et al.[46] They studied the role of amino-acids embedded in silica material, in the aim to develop a reproducible process to prepare solid monoliths (32 wt%) without the use of organic solvent and at controlled pH thanks to amino-acid induced pH (dependant of their isoelectric point). They found that with high glycine concentration (0.92 M) leading to pH 6.2, hydrolysis of tetramethoxysilane is slow down while condensation is speeded up. They proposed that amino-acids mediate the reaction by stabilizing both silanolate (Si-O^{-}) and silanol (Si-OH) species respectively by the ammonium and the carboxylic functions of amino-acids, through hydrogen bonds. This mechanism of reaction is quite different from the one we proposed, considering we are using completely different conditions of reaction. Indeed, in our case phosphate buffer controls the pH fixed at 7.4 and thus the kinetics of reactions are different between the formation of a solid monolith vs a hydrogel. Moreover, glycine is an additive in our case, with lower concentrations, just helping the sodium fluoride in its regular mechanism, catalysing both hydrolysis and condensation by coordination into silicon atom with both sides of the zwitterionic form. Our proposition is based on the high ability of the silicon atom to extend his coordination number in presence of nucleophilic species.[48]

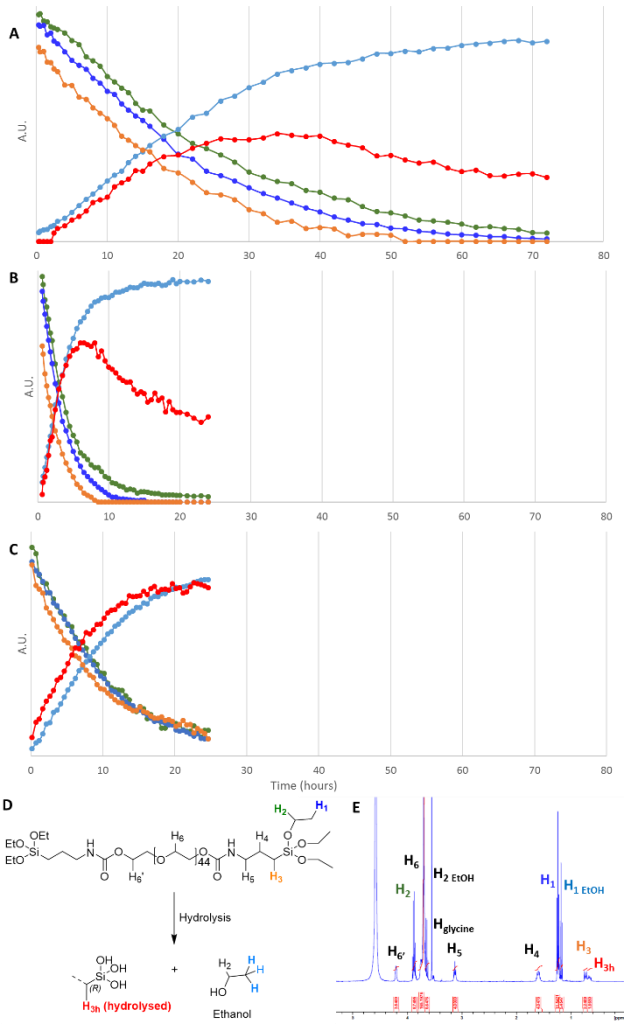

Figure 4. ^{1}H NMR signal integrations of bis-silylated PEG$_{2000}$ in D$_2$O/DPBS (10 %wt) as a function of time, divided by their theoretical number of equivalent protons. Experimental conditions: 37 °C , pH 7.45; (A) 0.1 mg/mL NaF; (B) 0.1 mg/mL NaF; 133 mM (10 mg/mL) glycine; (C) 0.1 mg/mL NaF; 133 mM methylamine; (D) proton attributions and attributed colours; (E) NMR signal attributions.

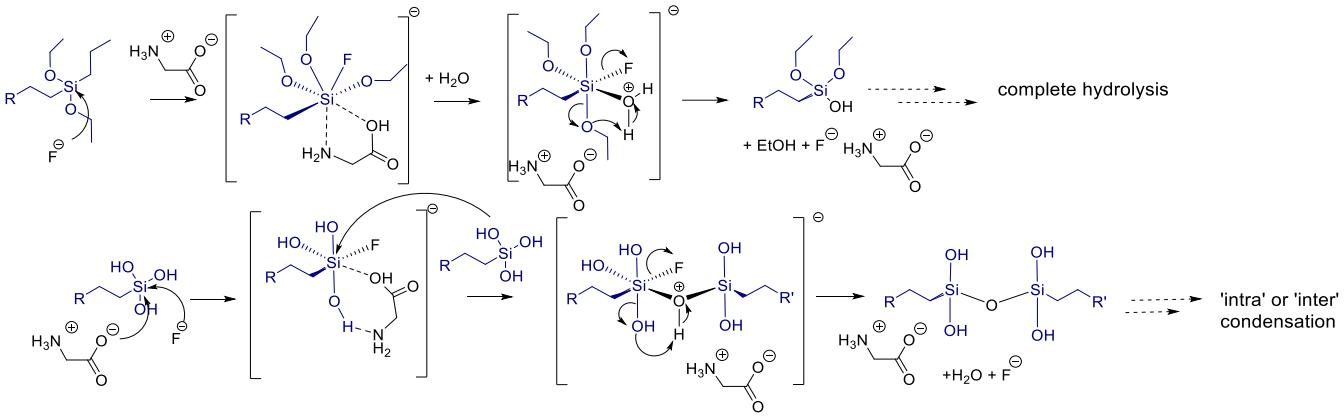

Scheme 3. Proposed mechanism of co-catalysis by F^- and glycine for hydrolysis and condensation in the sol-gel hydrogel formation.

Evolution of viscosity during catalysed gelation

From a macroscopic point of view, the catalyst had a huge influence on the gelation time. Evolution of the viscosity was recorded in DPBS either in the presence of 0.1 or 3 mg/mL NaF (2.38 mM and 71.5 mM respectively) or with 0.1 mg/mL of NaF in combination with 143 mM and 715 mM glycine respectively (light and dark green curves, Figure 6 and Table 2), at 37 °C. First, we observed that gelation time determined by tilting method corresponded to a measured viscosity of ~100 mPa.s. During condensation, oligomer species were formed and reacted together to give larger colloidal particles corresponding to the gel point found by rheology, at the intersection between G' and G" slopes. Then, these particles were cross-linked to reach a 'macroscopic gel point', corresponding to the gelation time determined by the tilting method (Figure 5). After this point, viscosity increased quickly. We determined that the 'ideal' printing window corresponded to a hydrogel viscosity comprised between 2500 and 4500 mPa.s, allowing the 3D printing of this hydrogel with a good retention of the shape, enabling extrusion and avoiding spreading.[10] Besides, the slope of the curve of viscosity as a function of time was calculated between the lowest and the highest limit of this interval; the smaller the value, the bigger amount of time usable for printing.

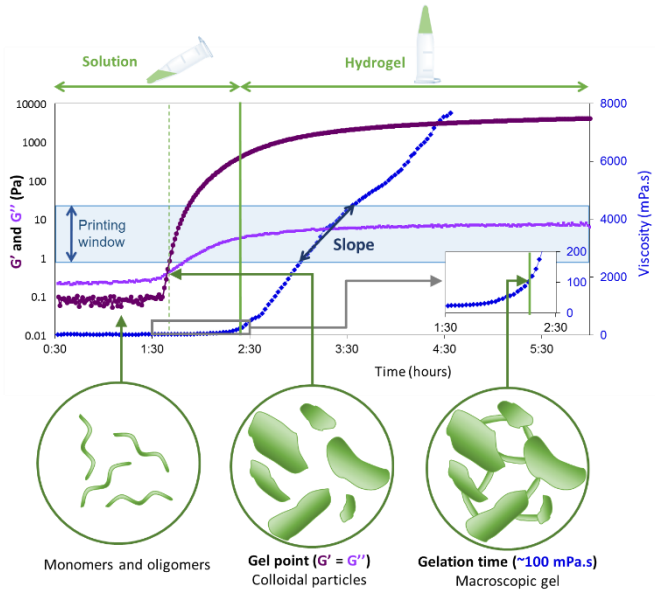

Figure 5. Representation of gel point and gelation time for hybrid PEG hydrogels.

As expected, the gelation time dropped from 53 to 2.25 hours when NaF was used at 3 mg/mL instead of 0.1 mg/mL, corresponding to a 23-fold decrease (Figure 6 and Table 2). The slope of the viscosity curve was also multiplied by 2.7-fold. Interestingly, the addition of glycine had only a limited impact on the slope of the curve (1.2-fold higher). However, the time to reach the 'macroscopic gelation point' was reduced by 3 to 4- fold upon glycine addition, yielding a tilting gel state within 17h30 in the presence of 143 mM glycine and 12h with 715 mM glycine.

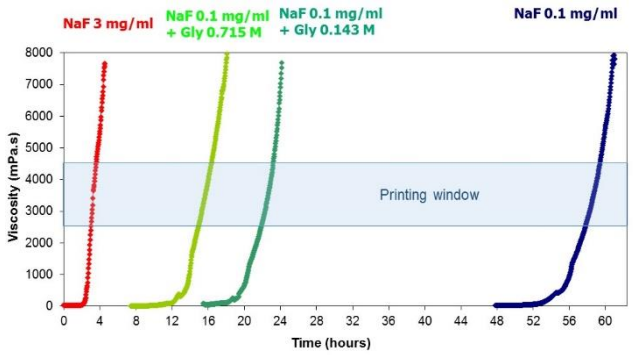

Figure 6. Viscosity of hybrid PEG hydrogels in DPBS (pH 7.4) at 37°C using different amounts of catalysts.

Table 2. Viscosity values of hybrid PEG hydrogels in DPBS (pH 7.4) at 37 °C using different amounts of catalysts.

Catalysts (mM)	Gelation time (100 mPa.s)	Time to reach 2500 mPa.s	Time to reach 4500 mPa.s	Slope (mPa.s/min)
NaF (71.5)	2h15	3h00	3h35	57.1
NaF (2.38)	52h52	57h46	59h23	20.8
NaF (2.38) + glycine (143)	17h28	21h52	23h12	25
NaF (2.38) + glycine (715)	11h58	14h55	16h20	23.5

Beside catalysts, numerous parameters do influence sol-gel reactions. The driving idea was to be able to adjust the sol-gel conditions to reach a suitable viscosity within a suitable windows frame to obtain a printable bioink. We already showed that a high concentration of the hybrid block speeded up the gelation by increasing the probability of reaction between silylated species.[15] For example, when PEG_{2000} was used at 20 wt% instead of 10 wt%, the gelation time was divided by two-fold (using 5 mg/mL NaF). However, the concentration was not a parameter we could easily play with because a minimum concentration was required to get a self-standing hydrogel. On the other side, the solubility and the nature of the hybrid molecule were limiting factors. For example, at the same 40 mM molar concentration, bis-silylated collagen-like peptide could not reach gelation compared to bis-silylated PEG_{2000}.[15,48]

Easier-to-tune parameters were investigated, including temperature, pH and buffer composition, but also the presence of cells. Hydrogels were prepared with the co-catalyst composition ([NaF] 2.38 mM and [H-Gly-OH] 143 mM) selected earlier.

Influence of temperature

As expected, temperature had a huge influence on the sol-gel polymerization (Figure 7 and Table 3). The increase in temperature made the reaction faster in the presence of 0.1 mg/ml NaF. The 'macroscopic gelation point' observed by the titling method happened after about 18 hours at 50 °C, 53 hours at 37 °C, 121 hours at 22 °C, and finally 220 hours at 7 °C. The slope of the curve was also dramatically affected, increasing with the temperature (e.g. 4.2 mPa.s/min at 22 °C and 20.8 mPa.s/min at 37 °C).

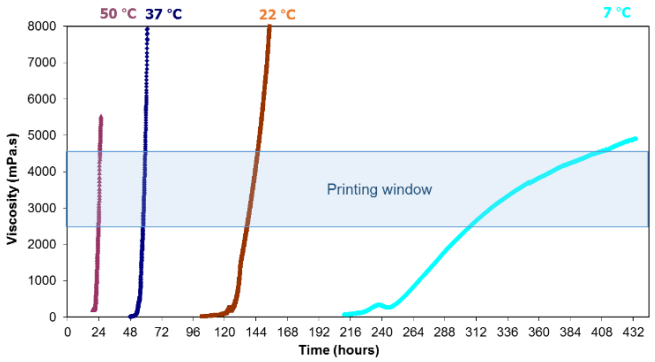

Figure 7. Viscosity of hybrid PEG hydrogels in DPBS (pH 7.4), in the presence of 0.1 mg/mL NaF, at different temperatures.

Table 3. Viscosity values of hybrid PEG hydrogels in DPBS (pH 7.4) in the presence of 0.1 mg/mL NaF, at different temperatures.

Temperature (°C)	Gelation time (100 mPa.s)	Time to reach 2500 mPa.s	Time to reach 4500 mPa.s	Slope (mPa.s/min)
50	<18h20	23h44	24h45	32.8
37	52h52	57h46	59h23	20.8
22	121h03	137h25	145h21	4.2
7	219h48	307h38	402h22	0.4

These results were particularly interesting in the light of handling a sol-gel based bioink (i.e. a hydrogel embedding cells). Indeed, the temperature could be adjusted between 40 °C and 20 °C, to tune the appropriate time of printing. In addition, hydrogels could be kept in the refrigerator (7 °C) up to 9 days before addition of cells, considerably slowing down the reticulation of the network and remaining in a low range of viscosity (i.e. for later use). This also means that the printing window could be enlarged by cooling the cartridge of the printer during the sol-gel based biofabrication. In the next set of experiments, we used a temperature of 37 °C, ideal for cell encapsulation.

Influence of the pH

As already stated, the sol-gel process was slow at pH 7 (Figure 1) due to the low hydrolysis rate.[11,19] However, we observed that even at pH values close to neutrality compatible with cell embedment, a small variation of pH greatly affected the gelation speed, even in the presence of catalyst. For example, gelation happened after 11h30 at pH 7.8, and after 17h30 at pH 7.4, i.e. 1.5 time-fold earlier (Figure 8 and Table 4). Indeed, on one hand the hydrolysis proceeded faster when moving far from neutrality, resulting in a lower macroscopic time of gelation. On the other hand, the slope of the viscosity curve was also significantly affected being 1.5 time-fold higher at pH 7.4 than at pH 7.8. This was explained by a slower condensation at higher pH. This observation has practical experimental consequences: the pH has to be fixed to get a reproducible gelation time, even in the presence of catalysts.

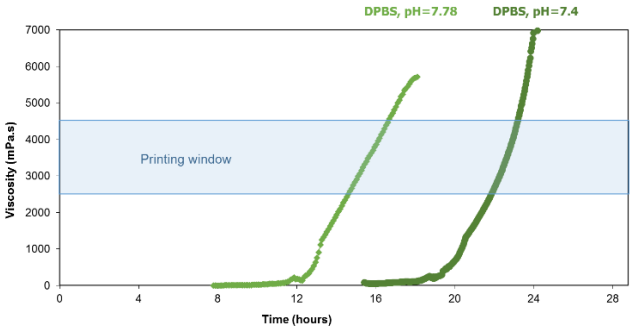

Figure 8. Viscosity of hybrid PEG hydrogels in DPBS at 37 °C in the presence of 0.1 mg/mL NaF and 143 mM glycine, at various pH.

Table 4. Viscosity values of hybrid PEG hydrogels in DPBS at 37 °C in the presence of 0.1 mg/mL NaF and 143 mM glycine, at various pH.

pH	Gelation time (100 mPa.s)	Time to reach 2500 mPa.s	Time to reach 4500 mPa.s	Slope (mPa.s/min)
7.4	17h28	21h52	23h12	25
7.78	11h33	14h37	16h40	16.3

Influence of the buffer

Culture media are complex mixtures of proteins, nutriments and salts. We can reasonably hypothesize that gelation goes faster as the complexity of the medium increases simply because the overall quantity of potential nucleophiles (e.g. amino acids, peptides) is also increasing. Hydrogels prepared in DPBS at pH 7.8 were compared with those obtained with chondrogenic medium (orange curve) or proliferative medium (blue curve) at the same pH (Figure 9, Table 5, see also supporting information for medium composition). As expected, gelation proceeded 1.05-1.2 time-fold faster in culture medium than in DBPS, the slope of the viscosity curve also increasing. The complexity of the medium composition made difficult the prediction of the acceleration of gelation time. Assays had to be performed for each cell culture medium.

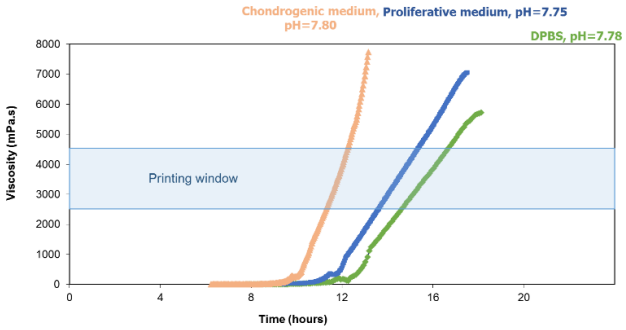

Figure 9. Viscosity of hybrid PEG hydrogels at 37 °C in different media in the presence of 0.1 mg/mL NaF and 143 mM glycine.

Table 5. Viscosity values of hybrid PEG hydrogels at 37 °C in different media in the presence of 0.1 mg/mL NaF and 143 mM glycine.

Medium	pH	Gelation time (100 mPa.s)	Time to reach 2500 mPa.s	Time to reach 4500 mPa.s	Slope (mPa.s/min)
DPBS	7.78	11h33	14h37	16h40	16.3
Chondrogenic medium	7.80	9h29	11h18	12h15	35.1
Proliferative medium	7.75	10h55	13h37	15h21	19.2

Influence of cells

It has already been reported that the presence of cells increased the viscosity of a physical bioink. Herein, we found that cells speeded up the sol-gel process. Viscosity measurements were performed in the presence of mMSCs (Figure 10 and Table 6) in proliferative medium at 37 °C and pH ~7.8. Gelation started 1.3 times-fold earlier than in absence of cells (8h30 instead of 11h). Besides, the slope was 1.7-fold higher. Taken together, these observations highlighted the influence of cells in both hydrolysis and condensation reactions. These results were in consistent with those obtained with complex media, as numerous functional groups present on cell surfaces as well as those found on proteins and small molecules released by cells, could behave as catalysts for the reaction.

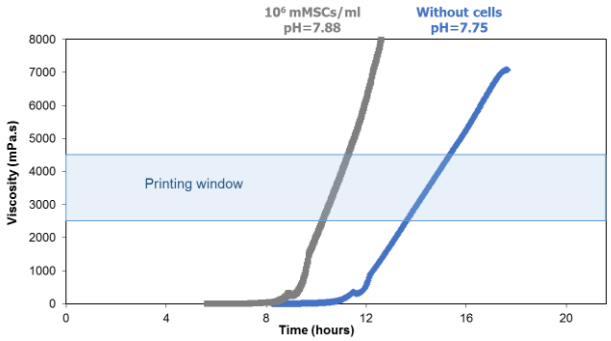

Figure 10. Viscosity of hybrid PEG hydrogels in proliferative medium (pH 7.8) at 37 °C, in the presence of 0.1 mg/mL NaF and 143 mM glycine, with or without cells (10^6 cells/mL).

Table 6. Viscosity values of hybrid PEG hydrogels in proliferative medium (pH 7.8) at 37 °C, in the presence of 0.1 mg/mL NaF and 143 mM glycine, with or without mMSCs (10^6 cells/mL).

mMSCs (10^6 /ml)	Gelation time (100 mPa.s)	Time to reach 2500 mPa.s	Time to reach 4500 mPa.s	Slope (mPa.s/min)
no	10h55	13h37	15h21	19.2
yes	8h30	10h15	11h17	32.3

Rheological characterization of hydrogels

To complete the study, rheological measurements were carried out during gelation of hydrogels prepared in the presence of 0.1 mg/mL NaF and 133 mM glycine, in DPBS at 37 °C or with 3 mg/ml NaF (Figure 11, green and red curves, respectively). Gel points were determined by the intersection of G' and G'' curves. A gel point of 7h50 was found for the hydrogel prepared in selected non-toxic conditions *vs*. 1h28 for the one catalysed with 3 mg/mL NaF. As expected (Figure 5), gel points were far from the 'macroscopic gelation time' obtained for those hydrogels (respectively 2h15 and 17h30). For these catalyst concentrations, the gel point was reached 5.2 time-fold earlier, while the 'macroscopic gelation time' was reached 7.8 time-fold earlier, probably due to the impact of NaF and glycine on the condensation rate. Nevertheless, both hydrogels reached a similar G' plateau at 4300 and 4100 Pa, indicating that whatever the catalyst used, the final rheological properties of hydrogels were similar. The storage modulus was converted into the Young's modulus (E) using the rubber elasticity theory, where $E = G' \times 2 \times (1+\nu)$, assuming a Poisson's ratio (ν) of 0.5 for bulk measurements of elastic hydrogel polymer networks. Young Moduli of 12.9 kPa and 12.3 kPa were determined.

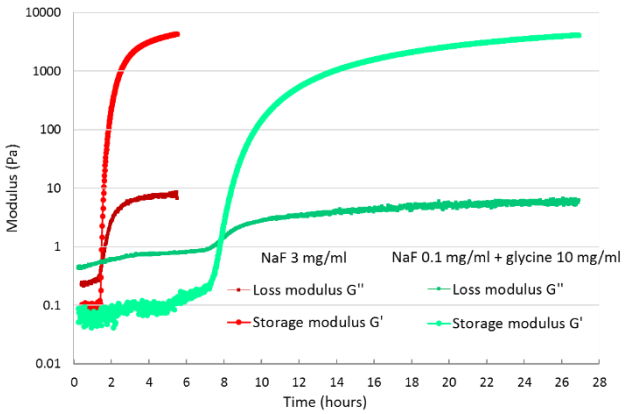

Figure 11. Rheology (time sweep) of hybrid PEG hydrogels at 37 °C in DPBS. Red curves in the presence of 3 mg/mL NaF; green curves in the presence of 0.1 mg/mL NaF and 10 mg/ml glycine.

Conclusions

Chemical hydrogels are obviously more difficult to handle than physical ones, as the establishment of covalent bonds is an irreversible process increasing the viscosity and the stiffness of the hydrogel in a time-dependent manner. Quick reactions such as photo-polymerization[49,50] have the advantage of being catalysed during the printing process (i.e. when the bioink flows out of the nozzle). It is not the case for sol-gel reactions, which have to be catalysed at physiological pH to yield hydrogels in a reasonable period. After screening more than 50 catalysts, the effectiveness of fluoride remained unmatched. We found that amino acids and glycine in particular, were able to speed up the gelation considerably in presence of low fluoride concentration, playing a role in hydrolysis and condensation of silyl groups. In cell-friendly conditions (37 °C in DPBS), gelation occurred after 53 hours when 0.1 mg/mL of NaF was used. This relative slowness can be advantageous while preparing bioinks for MSC-based engineering approaches. Indeed, cells can be poured into the precursor solution several hours before bioprinting, while temperature and addition of glycine can be used as an additional tuner to slow down or speed up the gelation, depending on the requirements of 3D printing. Beyond the use of the model hybrid PEG monomer, these data could be useful to optimize the 3D-printing of more complex sol-gel bioinks comprising more relevant silylated biomolecules such as peptides, proteins and oligosaccharides[51] in complex culture media.

Experimental Section

Experimental details (syntheses, characterization of compounds and experimental procedures) were provided on ESI.

Acknowledgements

This work was funded by the ANR (Agence Nationale de la Recherche), the French National Research Agency (ANR-16-CE18-0003).

Keywords: biocompatible catalysis • bioink • cell encapsulation • hydrogel • sol-gel process

[1] S. R. Husain, Y. Ohya, R. K. Puri, *Tissue Eng. Part A* **2017**, *23*, 471–473.
[2] K. Dzobo, N. E. Thomford, D. A. Senthebane, H. Shipanga, A. Rowe, C. Dandara, M. Pillay, K. S. C. M. Motaung, *Stem Cells Int.* **2018**, *2018*, 1–24.
[3] J. Jang, J. Y. Park, G. Gao, D.-W. Cho, *Biomaterials* **2018**, *156*, 88–106.
[4] J. D. Bronzino, D. R. Peterson, in *Biomed. Eng. Handb.*, **2015**, p. 114.
[5] X. Bai, M. Gao, S. Syed, J. Zhuang, X. Xu, X.-Q. Zhang, *Bioact. Mater.* **2018**, *3*, 401–417.
[6] Y. Wang, L.-Q. Cai, B. Nugraha, Y. Gao, H. L. Leo, *Curr. Med. Chem.* **2014**, *21*, 2480–2496.
[7] D. Bhatnagar, M. Simon, M. H. Rafailovich, in *Recent Adv. Biopolym.* (Ed.: F.K. Parveen), InTech, **2016**.
[8] O. Jeznach, D. Kołbuk, P. Sajkiewicz, *J. Biomed. Mater. Res. A* **2018**, DOI 10.1002/jbm.a.36449.
[9] L. Valot, J. Martinez, A. Mehdi, G. Subra, *Chem. Soc. Rev.* **2019**, 4049–4086.
[10] C. Echalier, R. Levato, M. A. Mateos-Timoneda, O. Castaño, S. Déjean, X. Garric, C. Pinese, D. Noël, E. Engel, J. Martinez, et al., *RSC Adv* **2017**, *7*, 12231–12235.
[11] E. J. A. Pope, J. D. Mackenzie, *J. Non-Cryst. Solids* **1986**, *87*, 185–198.
[12] L. L. Hench, J. K. West, *Chem. Rev.* **1990**, *90*, 33–72.
[13] A. M. Buckley, M. Greenblatt, *J. Chem. Educ.* **1994**, *71*, 599.
[14] T. Montheil, C. Echalier, J. Martinez, G. Subra, A. Mehdi, *J. Mater. Chem. B* **2018**, *6*, 3434–3448.
[15] C. Echalier, C. Pinese, X. Garric, H. Van Den Berghe, E. Jumas Bilak, J. Martinez, A. Mehdi, G. Subra, *Chem. Mater.* **2016**, *28*, 1261–1265.
[16] C. Echalier, S. Jebors, G. Laconde, L. Brunel, P. Verdié, L. Causse, A. Bethry, B. Legrand, H. Van Den Berghe, X. Garric, et al., *Mater. Today* **2017**, *20*, 59–66.
[17] A. Chiappone, E. Fantino, I. Roppolo, M. Lorusso, D. Manfredi, P. Fino, C. F. Pirri, F. Calignano, *ACS Appl. Mater. Interfaces* **2016**, *8*, 5627–5633.
[18] Y. Dong, J. Liang, Y. Cui, S. Xu, N. Zhao, *Carbohydr. Polym.* **2018**, *197*, 183–193.
[19] C. J. Brinker, G. W. Scherer, *Sol-Gel Science The Physics and Chemistry of Sol-Gel*, Academic Press, Inc., **1990**.
[20] A. Mehdi, C. Reyé, S. Brandès, R. Guilard, R. J. P. Corriu, *New J. Chem.* **2005**, *29*, 965.
[21] C. J. Brinker, *J. Non-Cryst. Solids* **1988**, *100*, 31–50.
[22] I. C. Tilgner, P. Fischer, F. M. Bohnen, H. Rehage, W. F. Maier, *Microporous Mater.* **1995**, *5*, 77–90.
[23] R. Winter, J.-B. Chan, R. Frattini, J. Jonas, *J. Non-Cryst. Solids* **1988**, *105*, 214–222.
[24] T. Tsutsui, N. Suzuki, M. Ohmori, H. Maizumi, *Mutat. Res. Lett.* **1984**, *139*, 193–198.
[25] J. H. Jeng, C. C. Hsieh, W. H. Lan, M. C. Chang, S. K. Lin, L. J. Hahn, M. Y. P. Kuo, *Cell Biol. Toxicol.* **1998**, *14*, 383–389.
[26] A. M. Khalil, A. A. Da'dara, *Arch. Environ. Contam. Toxicol.* **1994**, *26*, 60–63.
[27] J.-S. Song, H.-Y. Lee, E. Lee, H. J. Hwang, J. H. Kim, *Environ. Toxicol. Pharmacol.* **2002**, *11*, 85–91.
[28] E. Zeiger, M. D. Shelby, K. L. Witt, *Environ. Mol. Mutagen.* **1993**, *21*, 309–318.
[29] K. M. Delak, N. Sahai, *J. Phys. Chem. B* **2006**, *110*, 17819–17829.
[30] K. M. Delak, N. Sahai, *Chem. Mater.* **2005**, *17*, 3221–3227.
[31] J. P. Blitz, R. S. Shreedhara Murthy, D. E. Leyden, *J. Colloid Interface Sci.* **1988**, *126*, 387–392.
[32] R. J. P. Corriu, D. Leclercq, *Angew. Chem. Int. Ed. Engl.* **1996**, *35*, 1420–1436.
[33] R. J. P. Corriu, J. J. E. Moreau, P. Thepot, M. W. C. Man, *Chem. Mater.* **1992**, *4*, 1217–1224.
[34] X. Kästele, P. Klüfers, F. Kopp, J. Schuhmacher, M. Vogt, *Chem. - Eur. J.* **2005**, *11*, 6326–6346.
[35] J. D. Brennan, D. Benjamin, E. DiBattista, M. D. Gulcev, *Chem. Mater.* **2003**, *15*, 737–745.
[36] Y. A. Shchipunov, A. V. Krekoten, V. G. Kuryavyi, I. N. Topchieva, *Colloid J.* **2005**, *67*, 380–384.
[37] Y. A. Shchipunov, A. Kojima, T. Imae, *J. Colloid Interface Sci.* **2005**, *285*, 574–580.
[38] T. Liu, Y. Xu, *Mater. Chem. Phys.* **2011**, *129*, 1047–1050.
[39] S. Kawano, S. Tamaru, N. Fujita, S. Shinkai, *Chem. - Eur. J.* **2004**, *10*, 343–351.
[40] Y. A. Shchipunov, T. Y. Karpenko, *Langmuir* **2004**, *20*, 3882–3887.
[41] Y. Wei, J. Xu, H. Dong, J. H. Dong, K. Qiu, S. A. Jansen-Varnum, *Chem. Mater.* **1999**, *11*, 2023–2029.
[42] Y. Y. Meng, M. H. He, Q. Zeng, D. L. Jiao, S. Shukla, R. V. Ramanujan, Z. W. Liu, *J. Alloys Compd.* **2014**, *583*, 220–225.
[43] R. Norouzbeigi, M. Edrissi, *J. Am. Ceram. Soc.* **2011**, *94*, 4052–4058.
[44] T. Coradin, J. Livage, *Colloids Surf. B Biointerfaces* **2001**, *21*, 329–336.

[45] S. Wu, H. Cao, S. Yin, X. Liu, X. Zhang, *J. Phys. Chem. C* **2009**, *113*, 17893–17898.
[46] L. Kaßner, J. Kronawitt, D. Klimm, A. Seifert, S. Spange, *J. Sol-Gel Sci. Technol.* **2019**, *90*, 250–262.
[47] M. Chauhan, C. Chuit, R. J. P. Corriu, A. Mehdi, C. Reyé, *Organometallics* **1996**, *15*, 4326–4333.
[48] F. Carre, C. Chuit, R. J. Corriu, A. Fanta, A. Mehdi, C. Reye, *Organometallics* **1995**, *14*, 194–198.
[49] J. L. Ifkovits, J. A. Burdick, *Tissue Eng.* **2007**, *13*, 2369–2385.
[50] R. F. Pereira, P. J. Bártolo, *J. Appl. Polym. Sci.* **2015**, *132*, na-na.
[51] T. Montheil, M. Maumus, L. Valot, A. Lebrun, J. Martinez, M. Amblard, D. Noël, A. Mehdi, G. Subra, *submited* **2019**.

The sol-gel process requires nucleophilic catalyst to proceed in water at physiological pH. To reach good viability in silylated PEG hydrogels embedding cells, numerous compounds were assayed as catalysts or co-catalysts with NaF. The most effective one was found to be glycine, which assist the fluoride catalysis in both hydrolysis and condensation reactions. The effect of other reaction parameters such as temperature, pH, medium and cell presence was studied by viscosimetry.

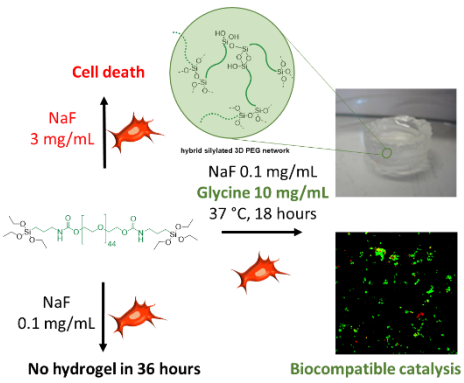

Laurine Valot, Marie Maumus, Titouan Montheil, Jean Martinez, Danièle Noël, Ahmad Mehdi and Gilles Subra**

Page No. – Page No.

Title